

Surface Protection and Improved Performance of Satellite Components as well as Mitigation of Space Environmental Pollution by Plasma Ion Implantation

M. Ueda, W. K. Takahashi, A. R. Marcondes, I. H. Tan, and G. Silva

Citation: [AIP Conference Proceedings](#) **1087**, 691 (2009); doi: 10.1063/1.3076887

View online: <http://dx.doi.org/10.1063/1.3076887>

View Table of Contents: <http://aip.scitation.org/toc/apc/1087/1>

Published by the [American Institute of Physics](#)

A promotional banner for AIP Conference Proceedings. The left side features a blue background with a water texture. The right side is a solid yellow triangle. Text is overlaid on both sections.

SUMMER SALE!

AIP | Conference Proceedings

30% OFF
ALL PRINT
PROCEEDINGS!

ENTER COUPON CODE
SUMMER2017

Surface Protection and Improved Performance of Satellite Components as well as Mitigation of Space Environmental Pollution by Plasma Ion Implantation

M.Ueda¹, W.K.Takahashi¹, A.R. Marcondes¹, I.H.Tan¹, G.Silva^{1,2}

¹National Institute for Space Research, São José dos Campos, S.Paulo, Brazil

²Technological Institute of Aeronautics, São José dos Campos, S.Paulo, Brazil

ABSTRACT

Three plasma processing systems based on PIII technique have been used in the improvement of surface properties of different materials important for aerospace and space applications. Metal plasma PIII of Al and Mg was used for surface protection of polymers used in space such as Kapton, Mylar and polyethylene. Al alloys were treated with nitrogen PIII for improved resistance to corrosion aiming at aerospace applications. A rigid polymer UHMWPE was also treated in a nitrogen PIII to produce a protective layer with DLC. Although not very light, SS304 stainless steel components are being used in a imaging camera in space, and some components made of this material showed endurance to vibration tests after nitrogen PIII, therefore being qualified for on-board application.

1. INTRODUCTION

Avoiding the surface erosion of materials in artificial satellites operating in low Earth orbit (LEO) is important for at least three reasons: 1) continued satisfactory operation of the satellite's components for its total lifetime, 2) self-contamination of the satellites exposed surfaces, 3) ever increasing and worrying space environmental pollution by slowly but steadily released materials or even microdebris from erosion of satellites surfaces. One obvious way to solve these critical problems is reinforcing the surfaces of the components against the attack by two major space environment factors in LEO: atomic oxygen (AO) and Ultraviolet (UV) radiation.

We have chosen the plasma immersion ion implantation (PIII) method to improve surface resistance of polymeric materials against AO and UV (as well as their synergetic effects) that are abundant in LEO, and in particular, demonstrated that implantation of Al into Kapton, Mylar and polyethylene provides surfaces that resist successfully the deterioration caused by these factors [1, 2]. Previous publications have proven the effectiveness of surface protection of these materials by ion implantation

[3]. Magnesium implantation was also carried out in the above polymers leading to the protection of their surfaces [4]. More recently, other authors [5, 6] have improved further Al and Si PIII treatments, obtaining thicker and more stable protection layers of those polymers.

Other materials being sent to space as components of scientific and commercial satellites have to endure the harsh space environment and maintain their integrity for the lifetime of the spacecraft. Some moving parts have to operate with high reliability, either once (stoppers or release mechanisms) or many times (bearings or springs) in space, where their replacements, in many cases, is impossible. Surface treatment of these critical components may become essential to guarantee the expected performance of the satellites for a long period.

Different materials for satellites under development in our institute are being treated by PIII for improved performance in space: besides the above mentioned polymers that were implanted with Al and Mg, Al alloys used for antennas for direct observation of the sun, painted surfaces for satellite temperature control, and rigid polymers, such as UHMPE, for future components structures, are being studied. Furthermore, improving the performances of satellites' internal parts used as components of imaging cameras (tested successfully after PIII treatment) and components for release mechanisms of solar cell pannels (made of NiTi memory form materials) are presently the major goals of our group concerning space applications of PIII surface modification technique.

2. EXPERIMENTAL

Three material processing systems based on the PIII technique have been used in this experiment. Metal arc plasma immersion ion implantation (MAPI³) of Al and Mg with low energy pulser (3-7 keV) has been carried out for treatments of flexible polymers such as Kapton, Mylar and polyethylene films [1, 7] with the major objective to protect the films against atomic oxygen (AO) and UV in space. For testing the treated films we used an oxygen plasma source that produced not only AO but also, O⁺, O₂⁺, UV and other ionic species of some contaminants [8]. The moderate energy (10keV < E < 20keV) PIII system (3IP-LAP) [9] used in present experiments was also used to treat with nitrogen light materials of interest for aerospace structure applications, as well as some components of an imaging camera to be used in the next generation of CBERS China-Brazil satellites [10]. A very high energy PIII (30keV < E < 75keV) system (3IPAE) was used for the bombardment of Al alloys, as well as rigid polymeric materials such as UHMWPE [11].

The protective properties of the treated surfaces against erosion by atomic oxygen were tested by submitting the treated samples to oxygen plasma produced by a 40 kHz parallel-plate capacitive

reactor¹⁵). Oxygen plasma was generated at a pressure of 27 Pa (200 mTorr, while base pressures were around 20 mTorr) and 200 W of power. The plasma density and electron temperature of these plasmas were typically $\sim 1 \times 10^{10} \text{ cm}^{-3}$ and 1-2 eV, respectively. Samples were weighed prior to exposure and at fixed 10 minute intervals during a total of about one hour exposure to the plasma.

For the surface analysis of the treated specimens we used XPS, a potentiostat system, Auger Electron Spectroscopy, SEM, RAMAN spectroscopy and a vibration system. Two XPS systems from different laboratories were used. For the flexible polymers we used an ESCALAB 220X from the Université des Sciences et Technologies de Lille. The Mg $k\alpha$ unmonochromatized line (1253.6 eV) was used for excitation. The spectrometer was operated in a constant pass energy mode ($E_{\text{pass}} = 40 \text{ eV}$) for recording high-resolution spectra. For depth profiles, the following conditions were used: argon gas pressure, 10^{-5} Pa ; ion energy, 3 keV, ion current, 1.27 μA , rastered area, 7.5x7.5 mm; angle of incidence (with respect to surface normal), 50°. Experimental quantification was obtained using the Eclipse software (VG Scientific). On the other hand, for the rigid polymer UHMWPE samples we used an XPS system from the Institute of Materials and Environmental Chemistry (IMEC), Hungarian Academy of Sciences (Kratos XSAM 800 spectrometer using Mg $K\alpha_{1,2}$ excitation).

Corrosion tests of the Al alloys were carried out in a potentiostat/galvanostat AUTOLAB, model PGSTAT30, with three electrode configuration inside an electrolytic cell. The cell contained a solution with 3.5% ppm of NaCl with pH equal to 6. The potentials were measured with respect to an Ag/AgCl reference electrode.

We also used x-ray diffraction (Philips 3410 diffractometer in the Seeman-Bolin 2 θ mode) for microstructure analysis and Auger Electron Spectroscopy (FISONS Instruments Surface Science, model MICROLAB 310-F, from IIBPMR-Dresden, Rossendorf) for elemental analysis and profiling of Al alloys and SS304 stainless steel. Morphology of some of the samples was analyzed by scanning electron microscopy (SEM) (JEOL model JSM-S310). Raman spectroscopy (Renishaw2000) with 514.5 nm Ar⁺ laser light was used for the characterization of the DLC formed on the surface of the rigid polymers. The PIII treated components of the imaging camera were tested in the vibration system (LDS-Ling Dynamic System, 160kN, 5-2kHz) at LIT (Integration and Test Laboratory) of National Institute for Space Research.

3. RESULTS

Firstly, results on flexible polymers will be reported. Kapton, Mylar and polyethylene films were bombarded with Al and Mg in the MAPI³ system. These films acquired very high resistance to erosion by oxygen plasma and UV after the treatment. Figure 1 shows the XPS depth profile of implanted Al in Kapton. As we can see from Fig. 2, a formed mixed layer of about 25nm containing Al, O, and C (with O and C coming from the base Kapton material) protected the film against exposure to the plasma consisting of O^+ , O_2^+ , and contaminants as well as UV radiation, produced in the oxygen plasma source. As we optimized the treatment conditions, the polymer surface became more resistant to the oxygen plasma. While the oxygen plasma source does not simulate the exact conditions of the LEO environment to which many satellites are subjected, it creates much more severe conditions. Hence we would expect that polymer materials with the Al PIII surface treatment would maintain their integrity for a long time in LEO.

Mg PIII was also applied to these polymers with good results, although not as good as with Al. Elemental depth profiles obtained by XPS are shown in Figure 3 for the three polymers studied. In the Kapton sample, about 25 nm of MgO coating is formed followed by a mixed layer with approximately the same thickness. Similar result were achieved on the polyethylene sample with a somewhat thinner coating (~ 15 nm) and thicker mixed layer (~ 20 nm). For Mylar (PET) samples on the other hand, a thinner coating of about 6-8 nm was deposited followed by ~2-4nm of mixed layer. This initially transparent sample presented a greyish and cracked coating after implantation in contrast to the PE sample which looked as transparent as an untreated sample, and the Kapton sample which presented a slightly darker coloration compared to a pristine sample.

Erosion resistance results, in terms of mass loss due to oxygen plasma exposure, are shown in Fig.4 for the implanted Kapton and Mylar samples, together with mass loss rates measured for untreated samples. It can be seen that the mass loss rates decreased significantly after Mg implantation for both Kapton and Mylar samples, with rates similar to the ones measured for Kapton samples implanted with aluminum [9]. It was not possible to test the polyethylene sample because the used PE films shrank almost immediately when exposed to the oxygen plasma, possibly because the film was bi-stretched during the fabrication process.

Next, results obtained for Al alloys will be shown. In Fig.5 we present the result of AES analysis performed in a sample of Al5052 treated with nitrogen PIII at 48 keV, 1.5 μ s pulse duration, 100Hz frequency, for a period of 1h. Nitrogen implantation with ~10% atomic percent peak concentration and penetration of up to around 80nm was achieved. A large concentration of oxygen was also implanted

(up to 50% atomic concentration) to a depth of near 60nm. It is clear from this result that insufficient amount of nitrogen was implanted because of two reasons: a low delivered dose and a very thick oxygen barrier to nitrogen influx, formed as a native layer and/or during the PIII processing.

Increased total treatment time and prior cleaning of the surface by argon bombardment should allow better implantation of nitrogen. This is necessary for a successful formation of AlN layer with good mechanical and tribological properties.

Using conditions of 75kV, 100Hz, 1.2 μ s pulse duration for 1h, we performed PIII of nitrogen in Al7475 for which the current was kept below 35A (to avoid arcing). The corrosion resistance of the implanted Al7475 was improved significantly with respect to the unimplanted alloy, as can be seen in Fig.6. X-ray diffraction showed formation of $Al_xN_yO_z$ and AlN in this case, which resulted in good anticorrosion properties of that alloy. This property is important for aerospace applications of such alloys.

As for the rigid polymer, it was possible to treat UHMWPE samples at 45keV and 70keV. At both energies the resulting samples showed dark black color which is an indication of chemical structure modification in the polymer's surface associated with hydrogen atoms removal from the polymeric chains and subsequent reorganization of the carbon atom links. For DLC formation the cross-linked bonds are the dominant change after ion implantation.

Figure 7 presents a Raman spectrum of a UHMWPE sample implanted at 45keV. Two shoulders can be clearly distinguished in the Raman spectrum that exhibit characteristics typical for the DLC, including a disorder peak (D peak) at 1350 cm^{-1} , and a graphite-like peak (G peak) at 1558 cm^{-1} . The two bands were fitted with two Gaussian functions and according to Marcondes et al [12] the sp^3/sp^2 ratio or the ratio of C- sp^3 hybridised bondings to C- sp^2 hybridised bondings are somewhat related to the intensities of D and G peaks, respectively. Using the Full Width at Half Maximum (FWHM) position of the G and D peaks and also the areas under the curves, we could obtain the peak integral intensity ratio, $I(D)/I(G)$, which is a quantitative indication of the fraction of C- sp^3 bondings formed by nitrogen ion implantation. In this case, the $I(D)/I(G)$ ratio was 0.72 which is reasonable in accordance with the estimated implanted dose of 10^{15} ions/ cm^2 . It is clear that it was possible to achieve such good result because of the high ion energy, since the pulse length was very short, leading to a relatively small implanted dose.

The implantation of UHMWPE with pulses of 70 kV has shown excessive heating problem since the temperature of the sample support increased too much, causing the melting of the surface touching the support and leading the polymer surface to crack in several points. No such problems were experienced for 45kV pulses.

Figure 8 shows the Raman spectrum of UHMWPE treated at the following conditions: 70kV, 100Hz, 1.2 μ s pulse duration for 2h. Despite of the melting of the sample surface in contact with the support, the dark black color of the samples after the treatment can be an indication that a high degree of DLC was formed at the polymer's surface. But that is not confirmed by the Raman spectrum. The ratio $I(D)/I(G)$ of 0.37 is an indication that probably only 30 to 40% of the C-C bonds are from C-sp³. The position of D peak in this case is located at 1276 cm⁻¹ but nothing can be inferred from this shifted position as the G peak is well located at 1560 cm⁻¹ and the shift of G peak is the only confident indication of sp³ content [13].

A series of XPS high resolution results after different etch times of the surfaces for samples treated under the conditions of 45kV, 100Hz, 1.5 μ s pulse, for 2hrs are shown in Figs. 9 and 10. As can be seen in Fig. 9, the N1s peak is centered at 399.5 eV. This can correspond to nitrile group (-C \equiv N) that has a N1s peak at 399.4 eV or can be the overlap of two peaks (398.3 eV from N-Csp³ and 400.2 eV from N-Csp²). In any case, the conclusion is that the implanted nitrogen ions are forming chemical bonds inside the polymeric structure, instead of forming nitrogen clusters. Figure 10 also indicates that with depth (with increased etching time) less N is available for bonding that is consistent with the regular nitrogen PIII profile. In terms of peak binding energies, the C1s peak is centered at 283.2 eV that is the same as the C1s peak of diamond (C-sp³) that indicates a high fraction of C-sp³ in the polymer surface. These DLC containing polymeric surface layers might prove useful either in the internal applications in satellites or aerospace use.

As an example of applications of PIII in real components for satellites, we report on important components of an imaging camera going on board the next CBERS satellites, made of stainless steel, that were treated with nitrogen PIII with moderate energy (10 – 20keV). The objective was to ensure a reliable operation of the focusing mechanism of the camera after the satellite launching procedure. Vibration tests performed in non-treated components for locking of the focusing device indicated that micro erosion takes place in the tip of that component (which leads to its malfunction). This effect was completely suppressed in the PIII treated version, and hence successful repeatable release/lock operations were possible after the vibration tests at LIT allowing the qualification of the camera for flight in the next CBERS missions.

Other treatments mentioned and not discussed in this paper are under way and their results will be reported elsewhere.

Acknowledgements

We are grateful for the AES measurements performed by Dr. H.Reuther from IIBPMR, Rossendorf-Dresden, Germany; for the XPS measurements by Dr. A. Andras from IMEC, Budapest, Hungary; for XPS profiles obtained by Dr. Gengembre from Université des Sciences et Technologies de Lille, France and for the vibration tests performed by Eng. M. Sakita from LIT/INPE. The components of the camera were provided by the Opto Eletronica company from S.Carlos, S.Paulo, Brazil.

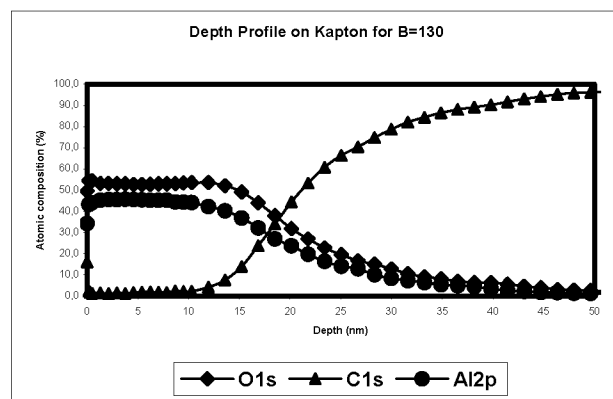


Figure 1. XPS depth profile of a Kapton sample biased to 7 kV in an Al magnetized plasma

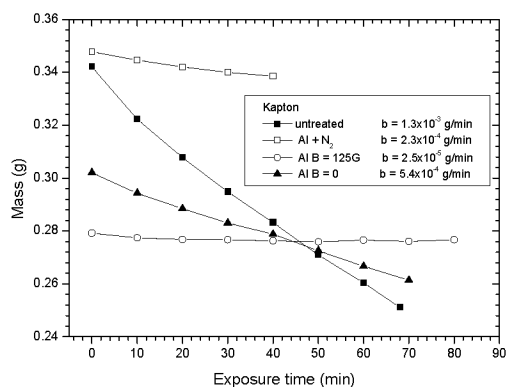
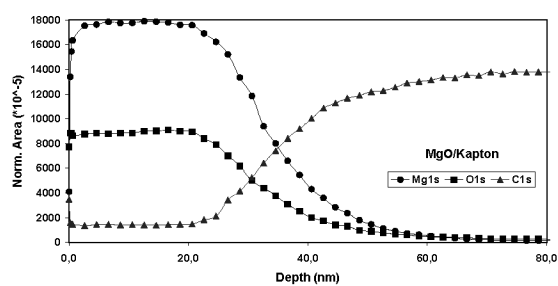
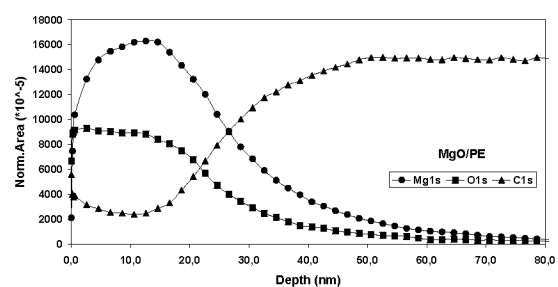


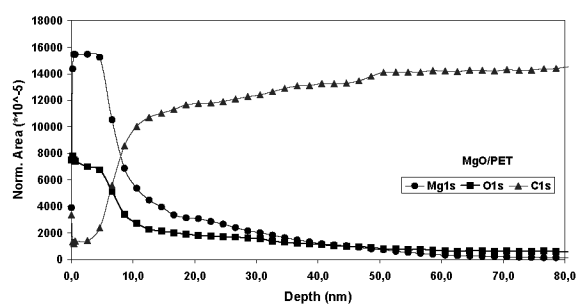
Figure 2. Mass losses of Kapton samples exposed to oxygen plasma: pristine sample (solid squares), sample treated in a magnetically confined plasma (open circles) and in an unconfined plasma (solid triangles), and indirect implantation by Al deposition followed by nitrogen implantation (open square)



(a)



(b)



(c)

Figure 3. XPS elemental depth profiles of Mg-implanted samples: (a) Kapton, (b) polyethylene and (c) Mylar (PET)

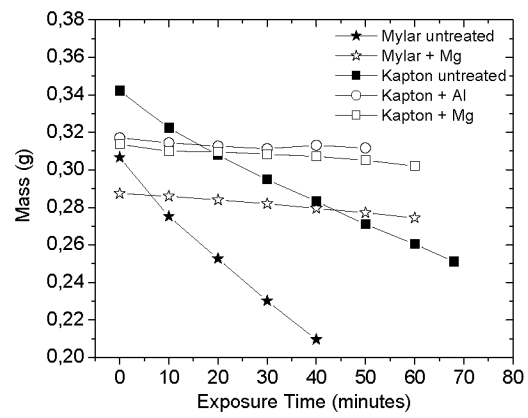


Figure 4. Mass loss as a function of exposure time to oxygen plasma for untreated (solid symbols) Kapton and Mylar samples and Mg implanted samples (open symbols). Aluminum implanted Kapton sample is also shown for comparison (open circle).

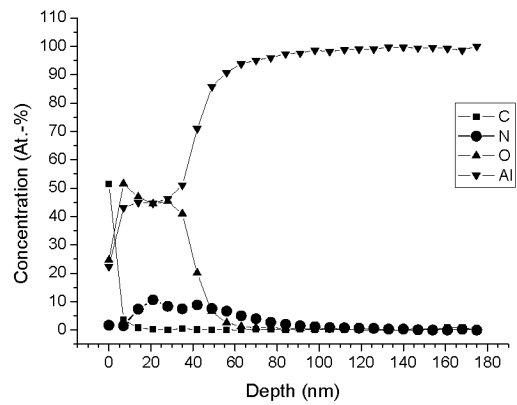


Figure 5. Auger depth profile analysis of implanted sample

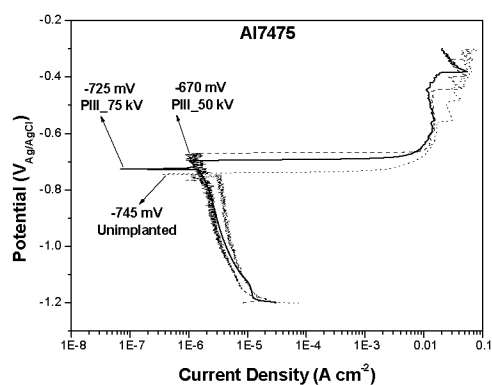


Figure 6. Polarization curves for different HVGD pulses

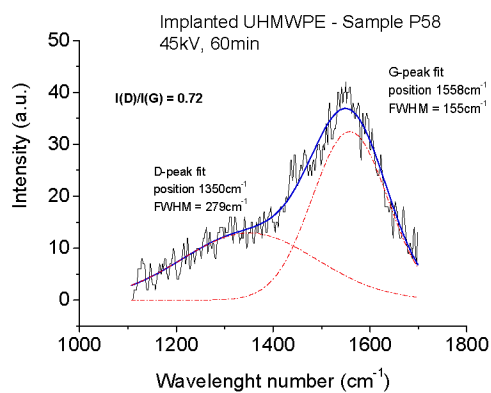


Figure 7. Fitted Raman Spectrum of UHMWPE implanted at 45 keV

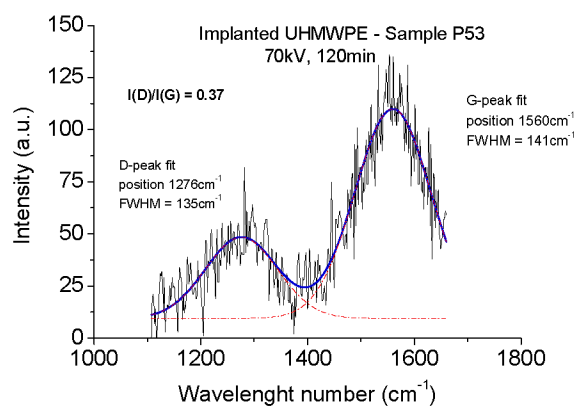


Figure 8. Fitted Raman Spectrum of UHMWPE implanted at 70 keV

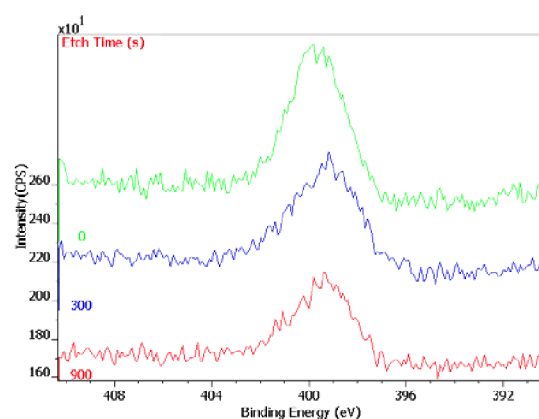


Figure 9. XPS high-resolution N 1s peaks of UHMWPE implanted at 45 keV, 120min for three different etch time

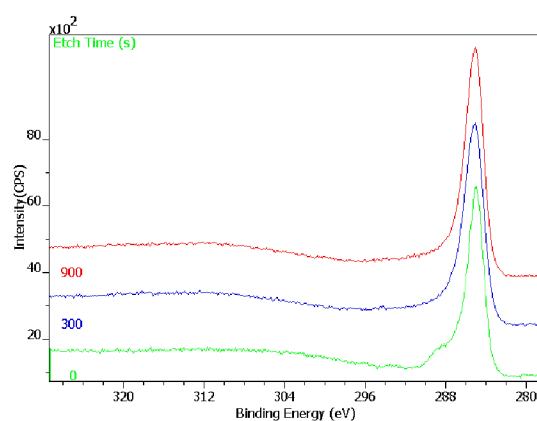


Figure10. XPS high resolution C 1s peaks of UHMWPE implanted at 45 keV, 120 min for three different etch time

REFERENCES

- [1] I.H.Tan, M.Ueda et al, Surf. Coat. Technol. 186 (2004) 234.
- [2] M.Ueda, I.H.Tan et al, Nucl. Instrum. Meth. B 206 (2003) 760.
- [3] Z. A. Iskanderova, J. I. Kleiman, Y. Gudimenko, et al, Nucl. Instrum. Meth. Phys. Res. B 148 (1999), 1090.

- [4] I.H.Tan, M.Ueda et al, Surf. Coat. Technol. 169 (2003) 379.
- [5] X.B.Tian, Y.X.Huang et al, 9th Int. Conf. PBII&D, 2007, Leipzig, Germany.
- [6] Y.X.Huang, X.B.Tian et al, Applied Surf. Science 253 (2007) 9483.
- [7] I.H. Tan, M.Ueda, R.S.Dallaqua, et al, Plasma Source Sci. and Technol., 11 (2002) 317.
- [8] I.H.Tan, M.Ueda, R.S.Dallaqua, L.Gengembre, et al, Plasma Processes and Polymers, 4 (2007) S1081.
- [9] M.Ueda, L.A.Berni, G.F.Gomes, et al, Journal of Applied Physics, 86 (1999) 4821.
- [10] T. M. Sausen, ISPRS Society, vol. 6. n.2, p. 27-28, June 2001
- [11] J.O.Rossi, M.Ueda, C.B.Mello, et al, submitted to IEEE, Trans. on Plasma Science, 2008.
- [12] A.R.Marcondes, M.Ueda, K.G.Kostov, et al, Brazilian J. of Phys. 34 (4B) (2004) 1667.
- [13] J. Robertson, Mat.Sci. Eng. Reports 37 (2002) 129.